Growth Strategies for Altermagnet(Mn_3Ga) for Spintronic Applications

Bhargav Naidu Palavalasa
Dept. of Physics
Indian Institute of Technology, Ropar
2022epb1242@iitrpr.ac.in

November 27, 2025

Abstract

This report presents a comprehensive study on the preparation of Mn_3Ga altermagnet alloys using arc melting techniques. Mn_3Ga is a binary Heusler alloy exhibiting remarkable magnetic properties including altermagnetism, characterized by fully compensated spins with broken parity-time (PT) symmetry and spin-split electronic bands. We detail the synthesis methodology involving arc melting followed by controlled thermal treatments, discuss the phase transformations between cubic, tetragonal, and hexagonal structures, and examine the resulting structural and magnetic properties. The work demonstrates that proper control of synthesis parameters enables the fabrication of different Mn_3Ga phases suitable for spintronic and quantum material applications.

1 Introduction

1.1 Altermagnetism: A New Class of Magnetic Materials

Altermagnetism represents an emerging paradigm in condensed matter physics, positioned between conventional ferromagnetism and antiferromagnetism [1, 2]. The discovery of altermagnetism addresses a fundamental gap in the classification of magnetic materials, providing a third basic magnetic phase beyond the traditional dichotomy of ferromagnets and antiferromagnets. The concept of altermagnetism emerged from theoretical predictions and experimental observations of unconventional spin physics in collinear antiferromagnets that could not be explained by conventional magnetic symmetry groups [1]. Traditional magnetic symmetry theory, based on coupled spin and real space transformations, failed to describe non-relativistic magnetic phases where spin and crystal momentum become locked in unique patterns.

The breakthrough came with the application of spin-group formalism, which considers decoupled transformations in spin space and real space [1]. This theoretical framework revealed the existence of a distinct magnetic phase combining zero net magnetization with momentum-dependent spin splitting - the altermagnetic phase.

1.1.1 Key Features and Technological Significance

Altermagnetism offers several unique features that make it particularly attractive for spintronic applications:

- **Zero Net Magnetization with Spin Splitting**: Unlike ferromagnets that have net magnetization and antiferromagnets that typically lack spin splitting, altermagnets combine the advantages of both - zero net magnetization eliminates stray fields while maintaining spin-split electronic bands.

- **Strong Spin-Coherence Effects**: The collinear spin arrangements in altermagnets preserve spin coherence over longer distances compared to relativistic spin-texture systems, making them ideal for spin transport applications.
- **High Transition Temperatures**: Many altermagnetic candidates, including Mn_3Ga-based systems, exhibit magnetic ordering at room temperature or above, enabling practical device applications.
- **Light Element Compatibility**: Unlike many spintronic materials that require heavy elements for strong spin-orbit coupling, altermagnets can be composed of abundant light elements while still exhibiting large spin splittings.

1.1.2 Unique Physical Properties

Altermagnets exhibit several extraordinary physical phenomena that distinguish them from conventional magnetic materials:

- **Anomalous Hall Effect without Net Magnetization**: The most striking feature is the appearance of large anomalous Hall effects in completely compensated magnetic systems, challenging the conventional understanding that net magnetization is required for such phenomena [6, 9].
- **Spin-Momentum Locking Protected by Crystal Symmetry**: Unlike relativistic Rashba or Dresselhaus systems where spin-momentum locking arises from spin-orbit coupling, altermagnets exhibit momentum-dependent spin splitting protected by crystal symmetries, leading to characteristic spin winding patterns.
- **Extraordinary Spin-Splitting Mechanism**: Altermagnets can exhibit spin splitting through two distinct mechanisms: conventional magnetic exchange interactions and, remarkably, through local anisotropic electric crystal fields [1]. This electric crystal field mechanism can generate spin splittings reaching 1 eV scale, comparable to ferromagnets but without net magnetization.
- **Current-Induced Magnetization Effects**: Altermagnets exhibit various forms of kinetomagnetism - current-induced magnetization in different orders (linear, odd-order, or even-order) [3]. This enables novel switching mechanisms for magnetic memory devices.

1.1.3 Research Motivation and Focus

The primary interest in altermagnetism stems from its potential to overcome fundamental limitations in conventional spintronic materials:

- **Elimination of Stray Fields**: The zero net magnetization eliminates problematic stray magnetic fields that limit device integration density in ferromagnetic systems.
- **Insensitivity to External Fields**: Altermagnetic devices are inherently robust against external magnetic field perturbations, a significant advantage for practical applications.
- **High-Frequency Operation**: The characteristic frequencies of antiferromagnetic dynamics are typically in the THz range, enabling ultrafast spin manipulation.
- **Novel Spin-Orbit Torque Mechanisms**: The unique symmetry properties enable efficient charge-to-spin conversion mechanisms that are prohibited in conventional magnetic materials.

The combination of these features makes altermagnets like Mn_3Ga promising candidates for next-generation spintronic devices, including ultra-dense magnetic memories, high-frequency oscillators, and energy-efficient computing architectures.

1.2 Symmetry Principles: Parity and Time Reversal

The fundamental symmetries governing altermagnetism are parity (P) and time reversal (T) operations:

1.2.1 Parity Symmetry (P)

Parity symmetry, or spatial inversion symmetry, transforms spatial coordinates as $\mathbf{r} \rightarrow -\mathbf{r}$. In momentum space, this corresponds to $\mathbf{k} \rightarrow -\mathbf{k}$. A system preserves parity symmetry if it remains invariant under this transformation.

1.2.2 Time Reversal Symmetry (T)

Time reversal symmetry reverses the direction of time ($t \rightarrow -t$). In quantum mechanics, the time reversal operator $\mathcal{T}$ acts on quantum states and has the fundamental property that $\mathcal{T}^2 = -1$ for half-integer spin systems, leading to Kramers degeneracy. For magnetic systems, time reversal flips spin directions: $\mathbf{s} \rightarrow -\mathbf{s}$.

1.2.3 PT Symmetry and its Breaking

The combined PT symmetry operation transforms both space and time simultaneously. For electronic states, PT symmetry links '+$\mathbf{k}$ with spin up' to '+$\mathbf{k}$ with spin down' states [3]. The breaking of PT symmetry is essential for altermagnetism, as expressed by:

$$[PT]\epsilon(s, \mathbf{k}) \neq \epsilon(s, \mathbf{k}) \tag{1}$$

This broken PT symmetry enables spin-split bands even in centrosymmetric crystals where individual P and T symmetries might be preserved.

1.3 Role of Spin-Orbit Coupling

Spin-orbit coupling (SOC) plays a crucial role in determining the nature of altermagnetic states:

- **Strong Altermagnets**: Exhibit spin-split bands through exchange coupling in the non-relativistic limit (zero SOC)
- **Weak Altermagnets**: Require non-zero SOC to manifest spin-split bands

The distinction arises from spin rotation symmetries, as discussed in Section 1.4.2.

1.4 Classification of Altermagnets

Altermagnets can be classified through multiple complementary schemes:

1.4.1 M-type, S-type, and A-type Classification

Based on their symmetry properties, altermagnets are categorized into three primary types [3]:

- **M-type**: Broken T symmetry with non-zero net magnetization due to orbital contributions. These belong to the ferromagnetic point group and exhibit linear anomalous Hall effects.
- **S-type**: Broken T symmetry with zero net magnetization and symmetric spin splitting. These do not belong to the ferromagnetic point group and can exhibit high odd-order anomalous Hall effects.

- **A-type**: Unbroken T symmetry with broken parity (P) and antisymmetric spin splitting. These can exhibit even-order anomalous Hall effects.

Additionally, **S/A-type** altermagnets exhibit both symmetric and antisymmetric spin splitting characteristics.

1.4.2 Strong vs. Weak Altermagnets

The distinction between strong and weak altermagnets is determined by spin rotation operations [3]. Consider a spin rotation operation $\mathbf{S}_n(\mathbf{r})$ that rotates all spins by $2\pi/n$ around the $\mathbf{r}$ axis without rotating the crystallographic structure.

- **Strong Altermagnets**: Have spin-split bands through exchange coupling even for zero SOC. These systems have *at most one* unbroken $\mathbf{S}_n(\mathbf{r})$ symmetry operation.
- **Weak Altermagnets**: Can only have spin-split bands with non-zero SOC. These systems have *two or more* unbroken $\mathbf{S}_n(\mathbf{r})$ symmetry operations.

Mathematically, for orthogonal x, y, and z axes, a magnetic system cannot have spin-split bands for zero SOC if it has two or more spin rotation symmetries out of $\mathbf{S}_n(x)$, $\mathbf{S}_n(y)$, and $\mathbf{S}_n(z)$.

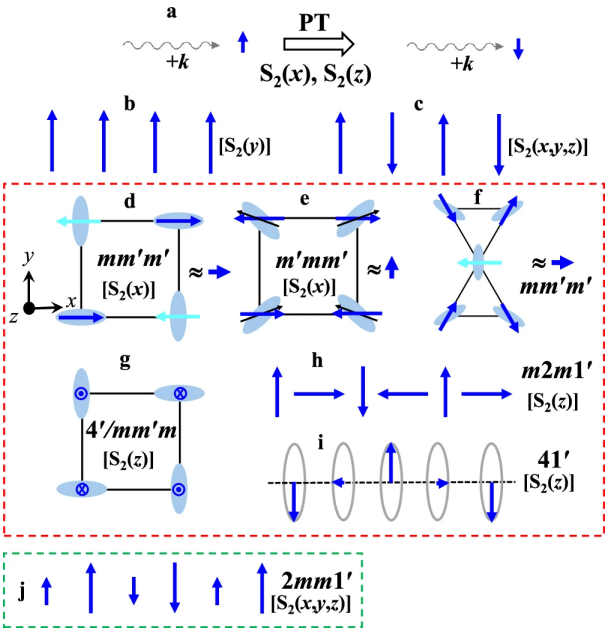

Figure 1: Classification of altermagnetic spin configurations based on symmetry properties. (a) PT, $S_2(x)$, or $S_2(z)$ symmetry operations link '+k with spin up' and '+k with spin down' states. (b-c) Conventional ferromagnetic and antiferromagnetic configurations (not altermagnets). (d-f) M-type altermagnets with broken time-reversal symmetry. (g) S-type altermagnet with broken time-reversal symmetry. (h-j) A-type altermagnets with unbroken time-reversal but broken parity symmetry. The presence of multiple spin rotation symmetries $[S_n(x, y, z)]$ (green box) indicates weak altermagnetism (spin splitting requires SOC), while a single spin rotation symmetry $[S_n(x)]$ (red box) indicates strong altermagnetism (spin splitting without SOC). Adopted from [3]

Key Results:

- All *collinear* M-type and S-type altermagnets are strong altermagnets

- All *collinear* A-type altermagnets are weak altermagnets
- Some *non-collinear* A-type altermagnets can be strong

1.5 Mn_3Ga as an Altermagnet

Mn_3Ga is a binary Heusler alloy that has attracted considerable attention as a multifunctional altermagnet material [8]. This compound exhibits multiple crystallographic phases with distinct magnetic properties:

1. **Cubic phase (γ-Mn)**: Disordered $L1_2$-type structure with collinear antiferromagnetic ordering
2. **Tetragonal phase ($D0_{22}$)**: Ordered structure with ferrimagnetic ordering and high magnetic anisotropy
3. **Hexagonal phase ($D0_{19}$)**: Two variants (α-phase and β-phase) with non-collinear antiferromagnetic ordering

The hexagonal β-phase of Mn_3Ga exhibits non-collinear antiferromagnetic spin configuration with 120° in-plane spin ordering on a triangular sublattice, making it a prototypical M-type altermagnet [8, 9]. This unique spin structure leads to large anomalous Hall effects, anomalous Nernst effects, and topological Hall effects at low temperatures [10].

1.6 Applications in Spintronics

The exceptional properties of Mn_3Ga make it highly promising for various spintronic applications [11]:

- Rare-earth-free permanent magnets (tetragonal phase with coercivity up to 21.4 kOe)
- Spin-transfer torque devices with predicted spin polarization up to 88%
- Antiferromagnetic spintronics utilizing non-collinear spin textures
- Magnetic tunnel junctions as pinned antiferromagnetic layers
- Topological Hall effect-based memory devices

1.7 Objectives of This Study

This report focuses on the systematic preparation of Mn_3Ga altermagnet alloys through arc melting techniques. The specific objectives are:

1. Establish optimal arc melting protocols for Mn_3Ga synthesis
2. Investigate phase transformation pathways through controlled thermal treatments
3. Characterize the structural and magnetic properties of different phases
4. Provide guidelines for tailoring Mn_3Ga phases for specific applications

2 Experimental Methodology

2.1 Materials and Precursor Preparation

High-purity elemental manganese (Mn, 99.999% wt.) and gallium (Ga, 99.999% wt.) were used as starting materials [8]. The stoichiometric composition was calculated based on the target phase:

$$\mathrm{Mn}_x\mathrm{Ga}_{1-x} \quad \text{where } x = 0.70 - 0.75 \text{ (70-75 at.\% Mn)} \tag{2}$$

For this study, we focus on the composition $\mathrm{Mn_3Ga}$ (75 at.% Mn, 25 at.% Ga), which corresponds to the stoichiometry for both tetragonal and hexagonal phases.

2.2 Arc Melting Process

2.2.1 Equipment Setup

The arc melting system consists of:

- Water-cooled copper hearth
- Tungsten electrode
- Controlled atmosphere chamber with argon gas inlet
- Vacuum pump system capable of reaching 10^{-3} to 10^{-1} Torr

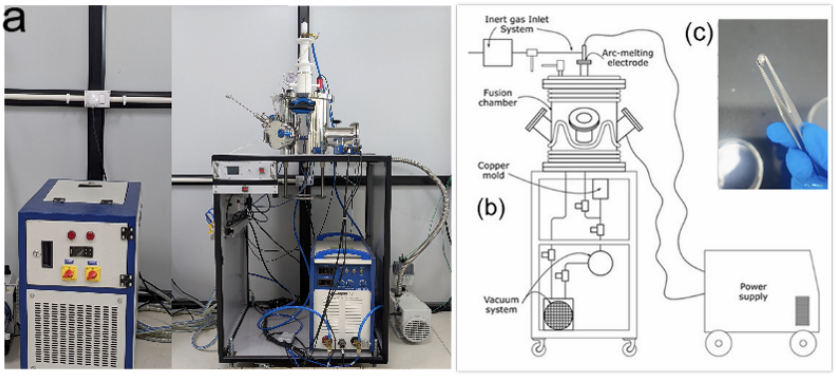

Figure 2: Arc-melting furnace (a) picture of the equipment, (b) drawing, and (c) example of one of the produced samples.

2.2.2 Synthesis Procedure

The detailed arc melting procedure is as follows [8, 14]:

1. **Chamber Preparation**: Evacuate the arc melting chamber to $\sim 10^{-3}$ Torr to remove residual air and moisture.
2. **Atmosphere Control**: Backfill with high-purity argon gas (99.999%) to a pressure of $\sim 10^{-1}$ Torr to prevent oxidation during melting.
3. **Initial Melting**: Place pre-weighed stoichiometric amounts of Mn and Ga elements in the copper hearth. Strike the tungsten electrode arc and melt a titanium getter button first to absorb residual oxygen.

4. **Alloy Formation**: Direct the arc onto the Mn-Ga mixture. The arc current should be gradually increased to ensure complete melting. Typical arc currents range from 30-50 A.

5. **Homogenization**: Flip and re-melt the ingot at least 3-5 times to ensure complete alloying and chemical homogeneity throughout the sample [13].

6. **Cooling**: Allow the molten alloy to solidify naturally on the water-cooled copper hearth, providing a cooling rate of $10^2 - 10^3$ K/s.

Note: The melting point of Mn_3Ga is approximately 1050-1100°C. Gallium has a low melting point (29.76°C) and high vapor pressure, so rapid melting is essential to minimize Ga loss through evaporation.

2.2.3 Weight Loss Compensation

Due to Ga evaporation during arc melting, a slight excess of Ga (typically 2-3 wt.% above stoichiometry) should be added to compensate for losses and achieve the target composition.

2.3 Melt Spinning (Optional Rapid Quenching)

For obtaining specific high-temperature phases, melt spinning can be employed as an alternative or complementary technique [8]:

- The arc-melted ingot is inductively re-melted in a quartz tube
- Molten alloy is ejected onto a rotating copper wheel
- Tangential wheel speed: 26 m/s
- Achievable cooling rates: $10^4 - 10^6$ K/s
- Results in ribbon-shaped samples with reduced grain size

The rapid cooling prevents phase transformations during solidification, enabling retention of high-temperature phases such as the disordered cubic structure.

2.4 Post-Synthesis Thermal Treatment

The as-cast samples undergo controlled thermal annealing to obtain desired phases:

2.4.1 Annealing Procedures

For Tetragonal $D0_{22}$ Phase [8, 12]:

- Starting material: Cubic phase obtained by arc melting or melt spinning
- Annealing temperature: 350-450°C
- Duration: 1-2 weeks for bulk samples, shorter for ribbons
- Atmosphere: Sealed evacuated quartz tubes ($< 10^{-3}$ Torr)
- Cooling: Furnace cooling to room temperature

For Hexagonal $D0_{19}$ β-Phase [8]:

- Starting material: Cubic or tetragonal phase

- Annealing temperature: 600-800°C
- Duration: Several hours to 1 week depending on starting phase
- Atmosphere: Sealed evacuated quartz tubes
- Cooling: Rapid quenching or controlled cooling
- Composition range: $Mn_{2.35}Ga$ to $Mn_{2.8}Ga$ (70-75 at.% Mn)

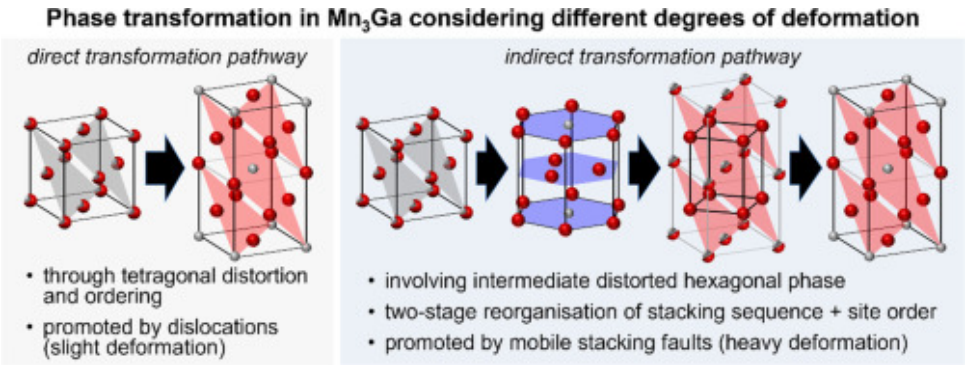

Figure 3: Phase transformation pathways in Mn_3Ga as a function of annealing temperature and time. Adopted from [8]

2.4.2 Phase Transformation Mechanism

The phase transitions in Mn_3Ga follow specific thermodynamic pathways [8]:

1. **Cubic → Tetragonal**: Ordering process where disordered cubic structure transforms to ordered tetragonal structure through atomic rearrangement at moderate temperatures (350-450°C).
2. **Cubic/Tetragonal → Hexagonal**: High-temperature transformation (> 600°C) involving significant structural reconstruction. Both cubic and tetragonal phases can transform to the hexagonal β-phase.
3. **Irreversibility**: The transformation to hexagonal phase is irreversible; cooling does not revert the structure back to cubic or tetragonal phases.

2.5 Characterization Techniques

2.5.1 Structural Characterization

X-ray Diffraction (XRD):

- Instrument: X-ray diffractometer with Cu K_α radiation ($\lambda = 1.5406$ Å)
- Scanning range: 2θ = 20-80°
- Step size: 0.02°
- Analysis: Rietveld refinement for lattice parameter determination

Scanning Transmission Electron Microscopy (STEM):

- High-angle annular dark field (HAADF) imaging
- Selected area electron diffraction (SAED) for phase identification
- Atomic resolution imaging for structural verification

2.5.2 Magnetic Characterization

Magnetometry:

- Magnetic Property Measurement System (MPMS, Quantum Design)
- Vibrating Sample Magnetometer (VSM, Lake Shore)
- Temperature range: 2-800 K
- Field range: 0-70 kOe

Differential Scanning Calorimetry (DSC):

- Heating/cooling rates: 10 K/min
- Atmosphere: Inert (argon)
- Purpose: Determination of magnetic transition temperatures

2.5.3 Transport Properties

Physical Property Measurement System (PPMS):

- Hall resistivity measurements
- Temperature-dependent resistivity
- Field-dependent magnetoresistance

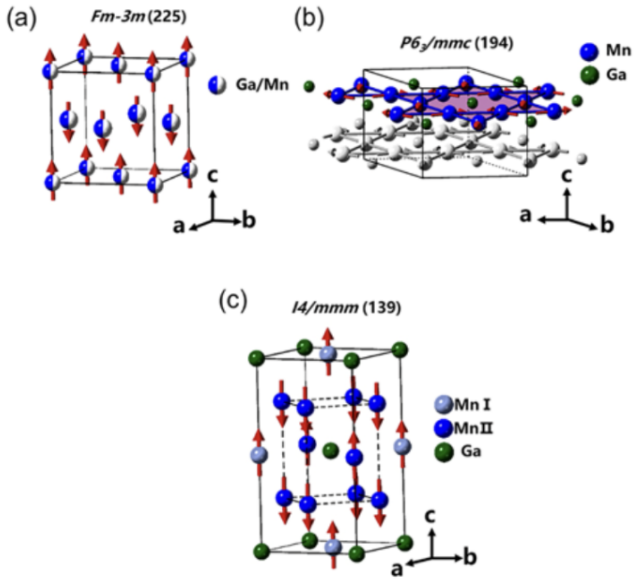

Figure 4: Crystal structures of Mn_3Ga: (a) cubic phase, (b) tetragonal phase, and (c) hexagonal phase. Adopted from [8]

3 Results and Discussion

3.1 As-Cast Material Characterization

3.1.1 Cubic Phase Properties

The arc-melted bulk Mn_3Ga typically crystallizes in the disordered cubic $L1_2$-type structure (γ-Mn phase). XRD analysis reveals:

- Space group: $Pm\bar{3}m$
- Lattice parameter: $a = b = c = 3.7786$ Å
- Magnetic ordering: Collinear antiferromagnetic
- Néel temperature: $T_N \approx 420$ K

The substitutional disorder in the cubic phase causes Mn atoms with antiparallel spins to cancel each other, resulting in antiferromagnetic ordering. This phase represents an S-type altermagnet with broken T symmetry and zero net magnetization [8].

3.1.2 Composition-Dependent Phase Formation

Melt-spun ribbons demonstrate composition-dependent phase formation [8]:

- $Mn_{3.2}Ga$ - $Mn_{2.9}Ga$: Pure cubic phase
- $Mn_{2.8}Ga$: Hexagonal phase
- $Mn_{2.6}Ga$ - $Mn_{2.7}Ga$: Cubic + Hexagonal mixed phases
- $Mn_{2.4}Ga$ - $Mn_{2.5}Ga$: Pure hexagonal α-phase

3.2 Tetragonal Phase Formation

3.2.1 Structural Properties

Low-temperature annealing (350°C, 2 weeks) of cubic Mn_3Ga yields the tetragonal $D0_{22}$ phase:

- Space group: I4/mmm
- Lattice parameters: $a = b = 3.9098$ Å, $c = 7.1011$ Å
- Magnetic ordering: Ferrimagnetic
- Curie temperature: $T_C \approx 700 - 820$ K

The tetragonal structure features two distinct Mn sublattices (Mn-I and Mn-II) with antiparallel magnetic moments, creating ferrimagnetic ordering. The c-axis is approximately twice the cubic lattice parameter, indicating an ordering transformation [8].

3.2.2 Magnetic Properties

The tetragonal phase exhibits remarkable magnetic characteristics:

- Large perpendicular magnetic anisotropy
- High coercivity: up to 21.4 kOe in pressed powder samples
- Saturation magnetization: $\sim 1.0\mu_B$/formula unit
- High spin polarization: theoretical 88%, experimental up to 58%

These properties make tetragonal Mn_3Ga promising for rare-earth-free permanent magnets and spin-injection devices [11].

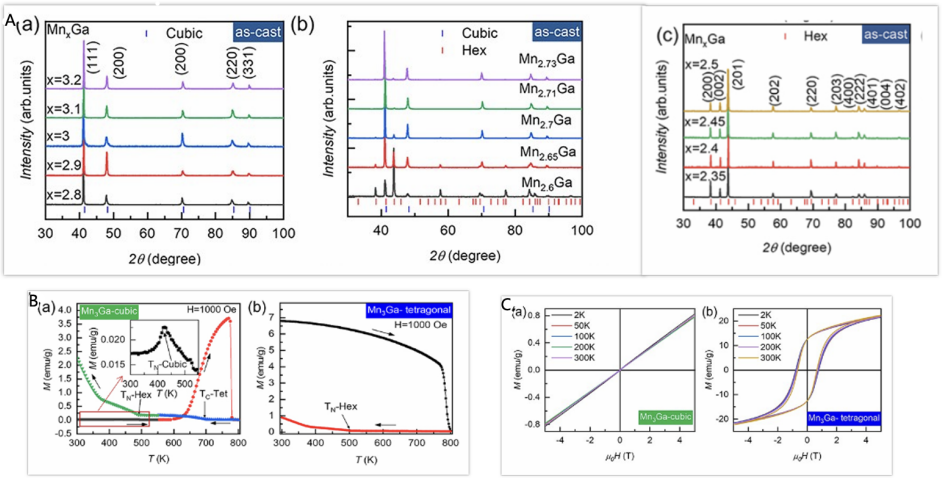

Figure 5: Structural and magnetic characterization: (A) XRD patterns, (B) temperature-dependent magnetization, (C) magnetic hysteresis loops. Adopted from [8]

3.3 Hexagonal β-Phase Synthesis

3.3.1 Formation Conditions

High-temperature annealing (600°C) successfully converts both cubic and tetragonal phases to the hexagonal β-phase:

- Space group: $P6_3/mmc$
- Lattice parameters: $a = b = 5.4084$ Å, $c = 4.3547$ Å
- Magnetic ordering: Non-collinear antiferromagnetic
- Néel temperature: $T_N \approx 490$ K

The hexagonal β-phase exhibits a triangular lattice with 120° in-plane spin ordering, characteristic of frustrated antiferromagnetism [8, 9].

3.3.2 Altermagnetic Properties

The hexagonal β-phase of Mn_3Ga represents a strong M-type altermagnet [3]:

1. **Broken PT Symmetry**: The non-collinear spin configuration breaks both parity and time-reversal symmetry.

2. **Spin-Split Bands**: Electronic structure calculations and experiments confirm momentum-dependent spin splitting without requiring spin-orbit coupling.

3. **Anomalous Hall Effect**: Large anomalous Hall conductivity $\sim 500\ \Omega^{-1}\text{cm}^{-1}$ at room temperature despite zero net magnetization [9].

4. **Topological Properties**: Topological Hall effect observed below 100 K due to non-coplanar spin components [10].

3.4 Phase Transformation Thermodynamics

DSC measurements reveal the phase transformation sequence [8]:

Cubic Phase Heating:

- 420 K: Néel temperature of cubic phase
- 600 K: Cubic $\rightarrow$ Tetragonal transformation begins
- 800 K: Tetragonal $\rightarrow$ Hexagonal transformation

Cooling Behavior:

- 490 K: Néel temperature of hexagonal β-phase
- No reverse transformation observed (irreversible)
- Possible γ-Mn precipitation in Mn-rich compositions

3.5 Altermagnetic Classification

Based on the symmetry analysis and magnetic properties [3], the Mn_3Ga phases can be classified as follows:

Table 1: Altermagnetic classification of Mn_3Ga phases

Phase	**Type**	**T Symmetry**	**P Symmetry**	**Strong/Weak**
Cubic	S-type	Broken	Unbroken	Strong
Tetragonal	M-type	Broken	Unbroken	Strong
Hexagonal β	M-type	Broken	Unbroken	Strong

All three phases are strong altermagnets, exhibiting spin-split bands without spin-orbit coupling due to the presence of only one spin rotation symmetry operation [3].

4 Applications and Future Perspectives

4.1 Spintronic Device Applications

The diverse properties of Mn_3Ga phases enable multiple applications:

1. **Tetragonal Phase**:
   - Rare-earth-free permanent magnets
   - Spin-injection sources for spin-transfer torque devices
   - Magnetic recording media with high anisotropy
2. **Hexagonal Phase**:

- Antiferromagnetic spintronics with large anomalous Hall effect
- Topological Hall effect devices for neuromorphic computing
- Magneto-optical devices utilizing Berry curvature effects
- Magnetic tunnel junction pinning layers

4.2 Advantages of Arc Melting Method

The arc melting synthesis route offers several advantages:

- Rapid melting minimizes Ga evaporation losses
- Complete alloying achieved through multiple re-melting cycles
- Scalable to bulk samples (several grams)
- Compatible with subsequent processing (melt spinning, annealing)
- Reproducible phase control through thermal treatment protocols

5 Conclusions

This report has presented a comprehensive methodology for the synthesis of Mn_3Ga altermagnet alloys via arc melting. The key findings and conclusions are:

1. **Synthesis Protocol**: Arc melting under controlled argon atmosphere with multiple re-melting cycles produces homogeneous Mn_3Ga ingots. Compensation for Ga evaporation is essential for achieving target stoichiometry.
2. **Phase Control**: The three principal phases (cubic, tetragonal, hexagonal) can be selectively obtained through controlled thermal treatments:
   - As-cast: Cubic disordered phase
   - 350-450°C annealing: Tetragonal ordered phase
   - 600-800°C annealing: Hexagonal β-phase
3. **Altermagnetic Nature**: All three Mn_3Ga phases exhibit altermagnetism with broken PT symmetry and are classified as strong altermagnets capable of spin-band splitting without spin-orbit coupling.
4. **Magnetic Properties**: The phases display distinct magnetic behaviors ranging from antiferromagnetism (cubic, hexagonal) to ferrimagnetism (tetragonal), with the hexagonal β-phase showing the most remarkable properties including large anomalous Hall effects and topological Hall effects.
5. **Application Potential**: The diverse properties of Mn_3Ga phases make them suitable for various spintronic applications, from permanent magnets (tetragonal) to antiferromagnetic spintronics (hexagonal).

The arc melting method combined with appropriate post-synthesis thermal treatments provides a reliable route for preparing Mn_3Ga altermagnets with tailored properties. The ability to control phase formation and magnetic ordering makes this material system highly promising for next-generation quantum and spintronic technologies. Future work should focus on scaling these synthesis methods for device fabrication and exploring the rich physics of altermagnetism in Mn_3Ga-based heterostructures.

References

[1] Šmejkal, L., Sinova, J., & Jungwirth, T. (2022). Beyond conventional ferromagnetism and antiferromagnetism: A phase with nonrelativistic spin and crystal rotation symmetry. *Physical Review X*, 12(3), 031042.

[2] Mazin, I. I. (2022). Editorial: Altermagnetism—A new punch line of fundamental magnetism. *Physical Review X*, 12(4), 040002.

[3] Cheong, S.-W., & Huang, F.-T. (2025). Altermagnetism classification. *npj Quantum Materials*, 10(38).

[4] Yuan, L. D., Wang, Z., Luo, J. W., Rashba, E. I., & Zunger, A. (2020). Giant momentum-dependent spin splitting in centrosymmetric low-Z antiferromagnets. *Physical Review B*, 102(1), 014412.

[5] Hayami, S., Yanagi, Y., & Kusunose, H. (2019). Momentum-dependent spin splitting by collinear antiferromagnetic ordering. *Journal of the Physical Society of Japan*, 88(12), 123702.

[6] Šmejkal, L., González-Hernández, R., Jungwirth, T., & Sinova, J. (2020). Crystal time-reversal symmetry breaking and spontaneous Hall effect in collinear antiferromagnets. *Science Advances*, 6(23), eaaz8809.

[7] Cheong, S.-W., & Huang, F.-T. (2024). Kinetomagnetism of chirality and its applications. *Applied Physics Letters*, 125(6), 060501.

[8] Song, L., Li, W., Lv, S., Xi, X., Zhao, D., He, J., & Wang, W. (2022). Tuning the structural, magnetic, and transport properties of Mn_3Ga alloys. *Journal of Applied Physics*, 131(17), 173903.

[9] Nakatsuji, S., Kiyohara, N., & Higo, T. (2015). Large anomalous Hall effect in a non-collinear antiferromagnet at room temperature. *Nature*, 527(7577), 212-215.

[10] Liu, Z. H., Zhang, Y. J., Liu, G. D., Ding, B., Liu, E. K., Jafri, H. M., ... & Wu, G. H. (2017). Transition from anomalous Hall effect to topological Hall effect in hexagonal non-collinear magnet Mn_3Ga. *Scientific Reports*, 7(1), 515.

[11] Balke, B., Fecher, G. H., Winterlik, J., & Felser, C. (2007). Hard magnetic properties of Mn_3Ga with a tetragonal structure. *Applied Physics Letters*, 90(15), 152504.

[12] Kirste, G., Decker, S., Gruner, M. E., Hu, M. Y., Zhao, J., Alp, E. E., ... & Pentcheva, R. (2023). Phase transformation in Mn_3Ga considering different degrees of cold deformation. *Acta Materialia*, 257, 119175.

[13] Crisan, O., Vasiliu, F., Mercioniu, I., Nicula, R., & Crisan, A. D. (2024). High magnetic performance in MnGa nanocomposite ribbons obtained by rapid quenching. *Materials*, 17(15), 3626.

[14] Liu, Z. H., Zhang, Y. J., Liu, G. D., Ding, B., Liu, E. K., Jafri, H. M., ... & Wu, G. H. (2018). Tailoring structural and magnetic properties of $Mn_{3-x}Fe_xGa$ alloys towards multifunctional applications. *IUCrJ*, 5(6), 794-800.